Development of a tomato pomace biorefinery based on a CO_2-supercritical extraction process for the production of a high value lycopene product, bioenergy and digestate.

Barbara Scaglia[a,*], Paolo D'Incecco[b,*], Pietro Squillace[a], Marta Dell'Orto[a], Patrizia De Nisi[a], Luisa Pellegrino[b], Alfondo Botto[c], Cristiano Cavicchi[d], Fabrizio Adani[a].

[a] *Ricicla Group labs- Dipartimento di Scienze Agrarie e Ambientali - Produzione, Territorio, Agroenergia- University of Milan, Milan, Italy;*

[b]*Dipartimento di Scienze per gli Alimenti, la Nutrizione, - University of Milan, Milan, Italy;*

[c] *Exenia Group, Via Carlo Borra 33/35, Pinerolo, Turin, Italy;*

[d] *Gruppo Cavicchi- XII Morelli, Ferrara, Italy.*

*** Corresponding Author**

Barbara Scaglia, Via Celoria 2, Milano, 20133- Italy, email: barbara.scaglia@unimi.it

Paolo D'Incecco, Via Celoria 2, Milano, 20133- Italy, email: paolo.dincecco@unimi.it

Abstract: Tomato peels and seeds (TP) are the most abundant canning industry waste actually used to produce biogas. TP is rich in lycopene (lyc) and represent a more sustainable feedstock than tomato fruits actually employed. It was therefore chosen as feedstock together with supercritical CO_2 extraction (SFE-CO_2) technology to develop a TP-SFE-CO_2 biorefinery, topic scarcely investigated. Two TP were tested and although TP-SFE-CO_2 parameters were the same, lyc recoveries depended by peel structure changes occurred during pre -SFE-CO_2 drying step. Higher moisture (102.7 g kg^{-1} wet weight) permitted 97 % lyc recovery and gave a water-in-oil emulsion as extract. Mass balance confirmed that lyc isomerisation did not cause lyc losses. After a significant oil extraction, exhaust TP showed a biodegradability 64% higher than the raw one, attributable to fibre structure disruption. The biorefinery proposed (SFE_CO_2+anaerobic digestion) determined positive economic revenue (+787.9 € t^{-1} TP) on the contrary of the actual TP management.

Keywords: lycopene, tomato pomace, anaerobic digestion, supercritical extraction, biorefinery

Abbreviations: tomato pomace (TP), lycopene (lyc), supercritical CO_2 extraction (SFE-CO_2), tomato pomace named S (S_{raw}), tomato pomace named A (A_{raw}), intermediate moisture (IM), biogas potential production test (ABP), S_{raw} exhaust fraction after TP-SFE-CO_2 (S_{exh}), A_{raw} exhaust fraction after TP-SFE-CO_2 (A_{exh}), broken and intact cell (BIC).

1. Introduction

The tomato industry is one of the most developed for vegetable processing at both European and world level (World Processing tomato council, 2016) and is responsible for the production of huge amounts of waste that creates a major disposal problem for the industry in terms of costs and environmental impacts (Urbonaviciene and Viskelis, 2017). Tomato peels and seeds (i.e. tomato pomace - TP) are the most abundant solid waste fraction, representing 2-3% of the starting weight of tomatoes. TP was usually composted but more recently started to be used as feedstock for anaerobic digestion (AD). AD is a biological process that took advantage by microbial activity to produce biogas, a renewable fuel, which consists of CH_4 (50 - 80 volume volume^{-1}) and CO_2 (Tani et al., 2006). Biogas production sector is currently on of the most sustainable energy production system and plays a key role in achieving the ambitious targets approved by the renewable EU energy directive (European Biogas Association, 2019). AD produces the digestate too, a solid stabilized biomass recognized as bio-based fertiliser by the new EU Fertiliser Regulation to replace synthetic N and P ones (Tambone et al., 2010; Riva et al., 2016; European Biogas Association, 2019).

High biodegradability is the most important biomass property to achieve high methane production. However, TP's homogenous composition and abundant bioactive components content imply that TP is the ideal biomass for further extraction of the valuable bioactive molecules and that the treated TP is only later used for bioenergy production. This fact, known as cascading use, led to an awareness of the need to develop a TP-based biorefinery to increase the productivity and efficient use of waste and by-product saving natural resources and reducing the waste production (Zero-waste principle) (Scoma et al., 2016).

TP is particularly rich in lycopene (lyc), the most powerful antioxidant carotenoid widely required by the cosmetic, food and pharmaceutical industries (Zunik et al., 2012). Thanks to its ability to act as

a quencher of singlet molecular oxygen radicals, lyc is one of ten carotenoids which are mainly marketed, with an economic value globally estimated of 1.5 USD billion on 2017 and a compound annual growth rate 2017-2022 (CAGR) of 2.3% (BBC Research, 2018).

Lyc is currently produced synthetically or extracted from tomato fruit cultivated for this purpose. Although the natural origin is a valuable market characteristic, actual production from fruits is no longer sustainable because of the agronomic cost, land consumption and food competition, so using TP represents an alternative source, making a transition from a first to a third generation production system (Urbonaviciene and Viskelis, 2017).

The lipophilic nature of lyc requires an apolar solvent such as ethylacetate to be extracted, which could leave traces affecting human health, especially when consumed daily (Zunik et al., 2012); in addition, the solvent evaporation step and final safe disposal increase the production costs (Nobre et al., 2009; Ollanketo et al., 2012; Kehili et al., 2017).

Already applied within the food industry, CO_2 supercritical technology (SFE-CO_2) is an alternative extraction method that avoids the solvent organic employment to develop greener manufacturers and healthier extract solvent free (Zunik et al., 2012; Attard et al.; 2015; Kehili et al., 2017), in which TP seed oil acts as CO_2 co-solvent and becomes the lyc solubilisation medium. Lyc health benefits are improved during SFE-CO_2 since the trans form is partially transformed into cis, that has higher oil solubility and bioavailability (Müller et al., 2011; Richelle et al., 2012).

With the aim to achieve maximum yield, several SFE-CO_2 extraction configurations have been tested and the lyc recovery evaluated, using as reference feedstock content (Ollanketo et al.; 2001; Topal et al., 2006) since TP-SFE-CO_2 was usually developed as a single-purpose process however this approach gave a partial understanding of the phenomena occurred under supercritical conditions such as extract losses, chemical conversion or degradation (Scoma et al., 2016).

Developing a complete biorefinery aims to maximise productions applying a series of processes by using the exhaust fraction as feedstock. To our knowledge, only two scientific papers have explored this possibility (Kehili et al., 2016; Allison et al., 2017) for TP and encouraging results were obtained when SFE-CO_2 was the first production step since the exhaust fraction is solvent-free and dried, therefore easily employable.

In this perspective, the quali-quantitative characterisation of the exhaust biomass becomes a fundamental aspect to drive the next production step and the mass balance approach is an indispensable instrument to verify process performance. By accounting for in-and-out biomass amount and composition it was possible to calculate theoretical extract characteristics (amount and chemical composition) that could be compared with experimental data to reach better understanding of the SFE-CO_2 effect.

The aim of this work was to develop a TP-SFE-CO_2 based biorefinery to produce TP extract rich in lyc, while the second step was AD to produce biogas and digestate. The SFE-CO_2 extraction was described through a complete TP-SFE-CO_2 mass balance approach never developed before, and the exhaust TP was characterised to evaluate the feasibility of using it for biogas and digestate production achieving a zero-waste approach.

2. Experimental Section

2.1 Materials

Two different TPs derived by the industrial transformation of tomato for industry cultivars named respectively S_{raw} and A_{raw} were collected from a full scale tomato canning plant located in northern Italy (OPOE facility in XII Morelli, Emilia Romagna Region, Italy) during activities performed from July

2017 to September 2017; about 30 kg of each biomass was brought to the laboratory for analytical characterisation.

2.2 Tomato pomace characterisation

2.2.1 Chemical Characterisation

Dry matter (d.m.) and fibre composition were determined as previously reported (Van Soest et al., 1991). Fibre analyses were performed for neutral detergent fiber (NDF), acid detergent fiber (ADF), and acid detergent lignin (ADL) to calculate the cell soluble (CS), cellulose (ADF - ADL) and hemicellulose (NDF - ADF) content (Van Soest et al., 1991).

The protein content was calculated based on the total Kjeldahl nitrogen (TKN) (The US Composting Council, 1997) multiplied by the coefficient 5.7 (Piyakina and Yunusov, 1995).

Before SFE-CO_2, S_{raw} and A_{raw} were partially dried in an oven at 50°C until they reached intermediate moisture (IM) contents of 50 g kg^{-1} wet weight (w.w.) and 100 g kg^{-1} w.w. respectively and the samples, named S_{rawIM} and A_{rawIM} were subsequently ground to 1-2 mm size. About 4 g of samples of S_{rawIM} and A_{rawIM} were extracted with 100 ml of hexane for 8 hours by using Soxhlet apparatus to measure oil content, which was calculated as the difference between the dried TP weight before and after extraction and retained as the reference to calculate the oil recovered by TP-SFE-CO_2. The Soxhlet extracts were used to carry out the subsequent lyc characterisation and TEAC test (see section 2.2.3). All the analyses were performed in duplicate. Statistical elaboration of this work were performed with the SPSS statistical software (version 20) (SPSS, Chicago, IL).

2.2.2 Lycopene quantification and characterisation

Lyc quali-quantitative characterisation was performed on an HPLC system (Agilent 1260 Infinity) equipped with a G1314F Agilent Uv/Vis spectrophotometer at 475 nm by using a C30 Develosil® rpaqueous column (5 µm, 250 x 4.6 mm). Hexane solution was injected at 25°C into the HPLC using as a mobile phase a mixture of methyl-tert-buthyl ether (306975, Sigma Aldrich, USA) (solvent A) and a solution of methanol + triethanolamine 0.1% (solvent B) (34860-M and 90278 respectively, Sigma Aldrich, USA) with a flow rate of 1.2 ml min^{-1}. The composition of the mobile phase was 15% A/85% B as the analysis began, to reach 55% A/45% B after 60 min and a final composition of 95% A/5% B after 65 min. All cis lyc isomer identification was based on the literature (Breitenbach et al., 2001; Urbonaviciene and Viskelis, 2017) and quantification was based on the trans-lyc analytical standard (L9879, Sigma Aldrich, USA).

2.2.3 Antiradical power assessment

The TP antiradical properties were assessed by performing the TEAC (Trolox Equivalent Antioxidant Capacity) assay by evaluating the 2,2-azinobis-3-ethyl-benzothialzoline-6-sulfonic acid ($ABTS^+$) radical cation decoloring reaction. $ABTS^+$ solution was prepared by mixing an $ABTS^+$ aqueous solution (7 mM) with potassium persulfate (2.45 mM, final concentration) and letting the mixture react in the dark at room temperature for 12–16 h. One hundred µl of extract was dissolved in 3.9 ml $ABTS^+$ solution, and 1 ml of the resulting solution was incubated for six minutes in the dark and then the solution absorbance was detected at λ=734 nm with a UV/visible Varian Cary 60 Spectrometer. Moreover, Trolox solutions (238813, Sigma Aldrich, USA) at different concentrations were used as standard. All the analyses were performed in duplicate.

2.2.4 Microscopic characterisation

S_{rawIM} and A_{rawIM} structures were investigated by scanning electron microscopy (SEM) and by optical microscopy. For SEM (Zeiss LEO 1430, Oberkochen, Germany) samples were gold-sputtered before observation at electron voltage of 5 kV, while thin TP sections (1µm thick) were stained with Toluidine Blue 1% in water and observed with a light microscope, Olympus BX-50 (Tokyo, Japan).

Cell wall ultrastructure was assessed using a transmission electron microscope (TEM) (Philips E208 transmission electron microscope, Philips Technology, Aachen, Germany). Samples were fixed in glutaraldehyde (2.5% v v^{-1} in 0.1 M sodium cacodylate buffer pH 7.2) (Agar Scientific, Stansted, UK) for 2 h at 4°C, then washed with 0.1 M sodium cacodylate buffer for 1 h and post-fixed in osmium tetroxide (EMS, Hatfield, USA) (1% in water, w v^{-1}) for 2 h. Samples were dehydrated in a series of ethanol solutions as described by D'Incecco et al. (2018), then embedded in Spurr resin (EMS, Hatfield, USA), and finally cured at 60°C for 24 h. Ultrathin (50–60 nm thick) sections were cut and stained with uranyl acetate and lead citrate (EMS, Hatfield, USA), both 0.2% in water (w v^{-1}).

2.2.5 Biological Characterisation

The biogas potential production test (ABP) was performed according to Scaglia et al. (2018). In brief, a 0.62 g d.m. sample, 37.5 ml of inoculum coming from digestate, and 22 ml of deionized water were put in 100-ml serum bottles. Digestate (d.m.= 34 g kg^{-1} w. w., Volatile Solid- VS= 740 g kg^{-1} d.m.) came from a full scale AD plant of North Italy; preliminary chemical characterisation (pH=8.33; Volatile Fatty Acids-VFA = 545 mg CH_3COOH l^{-1}; Total Alkalinity-TA= 1750 mg $CaCO_3$ l^{-1}; VFA/TA= 0.31; Ammonia= 1460 mg l^{-1}) confirmed the stable methanigen condition required to be employed as ABP test inoculum. The bottles were incubated at 37 ± 1 °C for 90 days. The biogas production was determined periodically and expressed as Nl kg^{-1} d.m. In addition to the samples, inoculum and glucose ABP tests were done and employed as blank and positive control respectively. Samples ABP

production were thus calculated as: cumulative ABP less blank ABP (ABP=26 Nl kg^{-1} d.m.). All the analyses were performed in duplicate.

2.3 Tomato pomace supercritical CO_2 extraction process

The S_{rawIM} and A_{rawIM} (1 kg wet weight, w.w.) were extracted in a pilot supercritical CO_2 extraction plant- SFE-CO_2 provided by Separeco S.r.l., Pinerolo (TO) Italy. The semi-industrial plant used was equipped with a 4.2 l extraction vessel, a 20 kWatt pump with a maximum flow rate of 90 kg CO_2 h^{-1}, and 3 separators (gravimetric, heated cyclonic, cooled cyclonic). CO_2 flow was monitored with a Coriolis mass flow meter.

Extracting conditions were set as follows: pressure 38 Mpa, temperature 80 ± 1°C and solvent ratio of 103 ± 4 kg CO_2 kg^{-1} d.m. The extractions were carried out until no further extract recovery occurred and the kinetics monitored at 10, 20, 30, 60, 100 kg CO_2 kg^{-1} w.w. S_{rawIM} and 15, 30, 45, 65, 90 kg CO_2 kg^{-1} w.w. A_{rawIM}. The SFE-CO_2 extracts were frozen for subsequent characterisation. The TP-SFE-CO_2 exhaust fractions (named S_{exh} and A_{exh} for the S_{rawIM} and A_{rawIM} respectively) were weighed and chemically characterised as previously described, to perform the TP-SFE-CO_2 mass balance.

2.4 TP-SFE-CO_2 extract microscopic characterisation

Extract composition was investigated using a LEICA DM R optical microscope. Sample drops were positioned on a microscope slide and observed without a cover glass under bright field (Perrechil et al., 2014). The emulsion was diluted with mineral oil and the images were acquired with a Leica EC3 camera and LAS V4.1 software.

In addition, emulsion microstructure was studied by using an inverted confocal laser scanning microscope (CLSM, Nikon $A1^{+}$, Minato, Japan). The specimen was stained with Nile Red to detect

neutral lipids. A stock solution (1 mg ml^{-1}) was prepared in 80% v v^{-1} DMSO (Sigma-Aldrich, St Louis, USA) and kept protected from light until use. Staining was performed at a concentration of 100 µg ml^{-1} and Nile Red was excited at 488 nm using an argon laser with the emission filter set at 520–590 nm. Separately, the staining with N-(lissamine rhodamine B sulfonyl) dioleoylphosphatidyl ethanolamine (Rh-DOPE), (Sigma–Aldrich, St. Louis, MO, USA and Avanti Polar Lipids Inc., Birmingham, England, respectively) was used to label phospholipids. A volume of 40 µL of Rh-DOPE solution (1 mg ml^{-1} in chloroform) was placed in a glass vial and the chloroform was evaporated under nitrogen to avoid possible artefacts caused by this organic solvent. Then 1 ml of extract was added in the vial and kept at room temperature for at least 1 h prior to observation by CLSM. Rh-DOPE was excited at 543 nm wavelength and emission detected between 565 nm and 615 nm. Observations were performed using a 63x (numerical aperture NA 1.4) oil immersion objective.

Image analysis was performed using Fiji (ImageJ software, Research Services Branch, USA) on maximum projection of CLSM z-stack images. Four images per sample were used and analyses were performed in duplicate. Microsoft Excel (Microsoft Corp., Redmond, WA) was used to calculate the size distribution of the water droplets in the extract.

3. Results and Discussion

3.1. Choice of TP-SFE-CO_2 extraction process parameters

Several lyc SFE-CO_2 processes tested different experimental conditions (Table 1) making difficult to identify which are fundamental extraction parameters to guarantee high lyc recovery (Baysal et al., 2000; Rozzi et al., 2002; Gómez-Prieto et al., 2003; Sabio et al., 2003; Topal et al., 2006; Vàgi et al., 2007; Ciurla et al., 2009; Nobre et al., 2009; Saldaña et al., 2010; Zhang et al., 2011; Machmudah et al., 2012; Honda et al., 2017; Vallecilla-Yepez and Ciftci, 2018; Hatami et al., 2019). Temperature and pressure are always reported for their effect on solvent density and solvent vs. matrix

interaction (Topal et al., 2006); although their averages were almost constant (temperature=77.4±13.7°C and P=37.3±7 MPa), lyc recovery was more variable (lyc recovery= 69±22% TP lyc) therefore these data were not enough to define extraction conditions. Flow rate and extraction-time (CO_2 flux= 11 ± 25 kg CO_2 h^{-1} and extraction time=211±103 min) were excessively changeable to identify reference to improve lyc recoveries (lyc recovery=73±18 % TP lyc and 72±20 % TP lyc for flow rate and extraction-time respectively).

Very few papers reported on the solvent ratio data, that is, the cumulative quantity of solvent required to extract the biomass. The average of 100±26.3 kg CO_2 kg^{-1} TP corresponded to a lyc recovery of 80±10 % TP lyc that was the highest found among all parameters (Table 1). This result suggested its importance to drive the TP-SFE-CO_2 performance, therefore this flow rate, together with corresponding temperature and pressure (average temperature= 82±4°C and average pressure= 36.8± 8.3 MPa) were applied in this work as follows: temperature= 80°C, pressure= 38 MPa, solvent ratio=103 kg CO_2 kg^{-1} TP (Table 1).

3.2 TP-SFE-CO_2 lyc kinetic extraction and peel morphology affect extraction yield.

The A_{rawIM} had a lyc content ten times more concentrated than the S_{rawIM} (Table 2). Lyc content in tomatoes varies in function of many factors like cultivated variety, agricultural practices adopted, ripeness stage and storage conditions, and has been reported to range from 2.5 to 670 mg 100 g^{-1} w.w. (Mayeaux et al., 2006; Akbudak et al., 2009). In addition, extractability of lyc is strictly linked to the TP moisture that at higher value (i.e. that of TP_{raw}) reduced lyc vs. solvent interaction while at lower content got vegetal tissue dehydration lowering permeability. A_{raw} and S_{raw} had very high moisture (Table 2) thus preliminary drying steps were needed to reach optimal intermediate moisture (IM) to perform SFE_CO_2. During drying pre-treatment lyc content of S_{raw} and A_{raw} were

monitored resulting similar for TPs for the same moisture content therefore the difference reported in Table 2 was attributable only to the modification occurred during pre-treatment.

In the raw tomato, trans lyc was the only form found (Shi et al., 1999), which was partially isomerized during industrial tomato processing and dehydration steps to get six cis molecules (Shi et al., 1999) (Table 2). For the S_{rawIM} the 9,13-cis-lyc, and 5,9-cis-lyc had the highest content followed by 15-cys-lyc and 7-cis-lyc while the A_{rawIM} showed a higher cis-lyc molecule number than the S_{rawIM} and the 7-cis-lyc and 5,9-cis-lyc were the most abundant molecules. The TP-SFE-CO_2 was able to extract 3.97 mg lyc kg^{-1} d.m. S_{rawIM} and 91.63 mg lyc kg^{-1} d.m. A_{rawIM} that corresponded to 73 % lyc S_{rawIM} and 97 % lyc A_{rawIM}, values almost different but within the ranges cited in the literature (Fig. 1; Table 1).

The lyc kinetics showed a first linear phase and a flatter second step (Fig. 1) associated with the lyc solvent solubility and lyc diffusion from the deeper tissues (Sabio et al., 2003; Vàgi et al., 2007). The first and second phases took longer for A_{rawIM} than for S_{rawIM}, implying that A_{rawIM} had a higher easily extractable lyc fraction in comparison with S_{rawIM} (Fig. 1).

Since the SFE-CO_2 extraction parameters were the same, biomass properties were assumed to affect the kinetics of extraction. Although data are not available for TP, a reliable model named “broken and intact cell-BIC” has been developed for seed oil SFE-CO_2 extraction (Fiori et al., 2009).

Basing on microscopic investigation, BIC considers biomass particles made up by several cell layers where, if the outer ones were partially broken during milling pre-treatment, the solute extraction was faster in comparison with intact cells located in the same coat and, above all, with those located in deeper layers (Vàgi et al., 2007; Fiori et al., 2009).

To verify this aspect, the TP peel fraction structure was investigated (Fig. 2). S_{rawIM} and A_{rawIM} peel remains had two main faces that corresponded to the external tomato fruit surface covered by

cuticle and to the parenchymatous cells layer located between the peel and pulp, in which polygonal wall structures were detected (Fig. 2 A, B, C, D). The peel faces observed did not show significant dissimilarities to explain the extraction trends, probably because TP peel had a more complicated structure than that of seeds (Fig. 2). Below the cuticle, there were a single-cell thick epidermal and two-four cutinized cell layers followed by the parenchymatous face (Crookes and Grierson, 1983) (Fig. 2 E, F). In comparison with fresh peel, S_{rawIM} and A_{rawIM} had enlarged intracellular spaces, cytoplasm that had become separated and evident wall thickness expansion; in fresh tissue, lyc is observable as crystals in the chromoplasts but in S_{rawIM} and A_{rawIM} it was not recognizable as a consequence of cytoplasm alteration (Fig. 2 E, F).

In comparison with the A_{rawIM}, the S_{rawIM} showed actual larger layer spaces. In the parenchymatous cells more evident wall shape widening occurred, in contrast with other cells positioned towards the cuticle surface. Structural damage to the peel was attributable to the thermal dewatering pre-treatment and to the duration of the process, which took longer for S_{rawIM} to reach the lower moisture content, causing very important morphological alterations (Table 2).

Ultrathin cross-sections' images were in addition analysed to better understand the modification occurred with the drying step (Fig. 2 G, H). At raw condition, cell wall was composed by cellulose microfibrils embedded in a hydrated matrix (water content of 75-90% w.w. cell wall) of hemicelluloses and pectins (Butchosa et al., 2019). TP cellulose crystallinity index of 34% meant that 66% of microfibrils had amorphous structure thus available to form bounds with other cell wall components over extended surface due to their big sizes (average thickness=32.24 nm, diameter of >45% microfibrils= 20-30 nm). Cellulose-OH were weakly linked to the other polysaccharides while very strong bounds were done with water that accumulated between microfibrils (Hubbe and Rojas, 2008; Szymańska-Chargot et al., 2017; Butchosa et al., 2019).

Upon drying procedure, the matrix collapsed above microfibrils and structure cell wall appeared thicker and more electron dense at the increasing of the water loss. Morphological changes corresponded to functional properties modifications such as lower porosity and higher rigidity of the cell wall that reduced in-out exchange capability across wall (Hubbe and Rojas, 2008; Szymańska-Chargot et al., 2017; Butchosa et al., 2019). S_{rawIM} cell wall was more electron-dense and 2-3 times thicker than A_{rawIM}, alterations explainable to the stronger dehydration degree (Li et al., 2014) (Fig. 2 G, H); the morphological difference supported the fact that S_{rawIM} in comparison with A_{rawIM} had lower attitude to the lyc extraction for the higher cell wall resistance that limited solvent way-in and lyc way-out cells in agreement with the kinetics (Fig. 1) (Saini and Keum, 2018).

3.3 TP moisture effect on the TP-SFE-CO_2 lycopene extraction yield

Some authors consider the TP water content to be an important parameter that influenced the lyc extraction and defined TP optimal moisture as between 46 g kg^{-1} w.w. TP and 228 g kg^{-1} w.w. TP (Ge et al., 2002; Shi et al., 2006; Zunich et al., 2012; Nobre et al., 2016). Due to the very high starting moisture, the TP dehydrating step was done until it reached "TP partially dried -TP_{IM}" with two different moisture contents that corresponded to the optimal range between medium (A_{rawIM}) and lowest (S_{rawIM}) values (Table 2)

A_{rawIM} gave very good lyc recovery confirming that the moisture level chosen gave the best TP-SFE-CO_2 performance. However, some authors described, for a TP moisture content similar to that of the S_{rawIM}, cell membrane lipid modification that makes it impermeable, reducing lyc recovery (Shi et al., 2006; Zunich et al., 2012; Nobre et al., 2016). Previous data highlighted how pre-treatment greatly modified the cell walls, contributing to affect lyc recovery; however, no data were reported about additional effects occurring during SFE-CO_2 extraction, during which water is converted to

steam that generates intracellular pressure able to achieve, as an extreme effect, cell wall rupture and tissue unravelling (Floros and Chinnam, 1998). With the aim of verifying this phenomenon, peel morphological changes occurring during TP-SFE-CO_2 were investigated (Figs. 2, 3). No significant modification was found for the S_{exh} cuticle face, while A_{exh} showed several scratches not present before (Fig. 2 A, B, Fig. 3 A, B). TP-SFE-CO_2 temperatures reduced waxy resistance and the hydrophobic nature of the waxes allowed them to avoid the steam, resulting in increased intracellular pressure and enhanced cuticle rupture (Li et al., 2014). Nevertheless process conditions were not the only cause of this effect, that occurred only for A_{rawIM} probably due to the higher water content that in the steam state created enough intracellular pressure to scratch the outer layer.

Parenchymatous faces (Fig. 3 C, D) also showed evident tissue disorganization if compared with the starting biomass, which was attributable to the steam effect (Fig. 2 C, D, Fig. 3 C, D). A_{exh} had several empty and broken cells with thin walls; on the contrary, S_{exh} cells appeared almost full showing very large thick walls that occupied most of the face surface.

Cross section images confirmed SEM data (Fig. 3 E, F). Both peel structures appeared less dense than the corresponding TP_{rawIM} with dissimilar cellular fullness intensity in agreement with lyc recoveries (Fig. 2 E, F). S_{exh} had cell wider walls than S_{rawIM} and showed a progressive thickness reduction from the parenchymatous towards the cuticle face; for the same biomass cell fullness was maximum for epidermal layer below the cuticle and decreased in the direction of the parenchymatous face, indicating a different extractability tendency of the layers. A_{exh} layers' cells appeared differently, seeming almost empty and showing similar cell wall conformation and interlayer space dimensions, suggesting a similar extractability for all cell layers. This last difference can be supposed to depend on the A_{rawIM} cuticle scratches that improved cell solvent accessibility and solute exiting from cells more proxy to the cuticle, improving lyc recovery.

3.4 TP-SFE-CO_2 effect on extract physical, chemical composition and antioxidant power

The extracts accounted to 63.6 g kg^{-1} S_{rawIM} and 110.8 g kg^{-1} A_{rawIM} that represented 67 g kg^{-1} d.m. S_{rawIM} and 123.5 g kg^{-1} d.m. A_{rawIM}. The TP_{rawIM} and TP_{exh} comparison gave indications about the fractions' nature (Table 2), that were composed of oil for TP_{rawIM} and oil plus water for the A_{rawIM} (Table 2) meaning that S_extract and A_extract have different physical compositions.

With the aim to check extract quantity and composition, theoretical whole oil and water amounts were calculated by accounting for in-and-out TP weight (A_{rawIM}=S_{rawIM}= 1000 mg and S_{exh}= 936.4 g kg^{-1} S_{rawIM} and A_{exh}=890 g kg^{-1} A_{rawIM}) and oil and water contents (Table 2, 3). Theoretical extracts amounts were of 103.2 g kg^{-1} S_{rawIM} and 112.8 g kg^{-1} A_{rawIM}, derived together by the water plus oil. Experimental and calculated data fitted very well for the A_extract that was composed of water: oil in the proportion of 70 % : 30 % weight A_extract. S_extract was theoretically composed of water and oil (water : oil being 29 %: 71 % weight S_extract) but the experimental amount measured was less than that calculated, for a quantity that corresponded to a water fraction probably retained in the SFE-CO_2 plant and in any case statistically negligible (Table 2).

Microscopic investigation confirmed that S_extract was oil and A_extract was oil in which there were water droplets (Fig. 3). The difference was probably due to the available water amount that was higher for A_{rawIM} and was thus co-extracted with oil during TP-SFE-CO_2 (Shi et al., 2009). Based on the drop measurement (water droplet size in the range 0.7 μm - 38.90 μm, with a mean diameter of 2.89 ± 3.60 μm) (see Supplementary Material) A_extract was classified like a water in oil emulsion (W/O) of which the steady state was guaranteed by emulsifier molecules identified as phospholipids forming a layer around the water droplets (Fig. 3).

Lyc content was of 63 mg kg^{-1} and 833 mg kg^{-1} for S_extract and A_extract respectively and had a different trans:cis ratios (Table 3) with higher cis content in comparison with TP_{rawIM} lyc. This change is called isomerisation and is fairly frequent when trans lyc is kept at 70-100°C (Yi et al., 2009) (Table 1, 3). Cis isomers had amorphous structure and higher lipophilicity than trans, therefore were more bioavailable, improving the extracts' health beneficial properties (Shi et al., 2009). From a quantitative point of view previous works considered isomerisation a degradative event that increased molecules' instability until they determined lyc loss (Urbonaviciene and Viskelis, 2017; Mutsokoti et al., 2017). In this work, thanks to the mass balance approach, lyc losses were excluded since the whole of the lyc extracted was calculated (3.84 mg kg^{-1} d.m. S_{rawIM} and 93.7 mg kg^{-1} d.m. A_{rawIM}) in agreement with the experimental values (Fig. 1); the same approach allowed us to calculate that very similar trans lyc fractions (14% trans lyc and 21% trans lyc amounts for the S_{rawIM} and A_{rawIM} respectively) were isomerized (Shi et al., 2009). The results seem to confirm that the chemical reaction depends above all on the temperature adopted: nevertheless, those data combined with the different lyc recovery rates, that depended on biomass properties, gave extracts with lyc compositions which were very dissimilar (Table 3).

Besides lyc concentration, the extracts' most important property for subsequent employment in the cosmetic, nutraceutical and food sectors is antioxidant power. A_extract TEAC was three times higher than S_extract in agreement with its higher lyc concentration (Table 3) and were together comparable with other lipophilic tomato extracts and powerful antioxidant molecules such as tocopherol (Longo et al., 2012).

The extracts' antioxidant power depended on the TP_{rawIM} content and on the extraction process that was carried out at high temperature to increase lyc recovery while destroying other thermolabile molecules, a process which might have decreased the antioxidant properties (Shi and Maguer, 2000; Vàgi et al., 2007; Egydio et al., 2010; Liu et al., 2011; Kehili et al., 2016; Mutsokoti et al., 2017).

Effectively TP_{rawIM} had a very different lyc content (Table 2) but similar TEAC attributable to the whole antioxidant content (i.e. other carotenoids, lipids, tocopherols) (Shi and Maguer; 2000); however at the end of the TP-SFE-CO_2 extraction, TEAC were lower than those of the starting TP and more strictly linked to lyc (Table 1). With the aim to quantify whether the process effectively affected the antioxidant properties, mass balance was applied. Expected TEAC were of 60.9 mmol kg^{-1} S_extract and 63.9 mmol kg^{-1} A_extract that are respectively 80 % and 57% lower than those experimentally measured (Table 2, 3), giving numerical evidence of the supercritical extraction's huge TEAC reduction; moreover the high effect on S_{rawIM} in comparison with the A_{rawIM} could be partially explained by its lower extractability.

3.5 TP-SFE-CO_2 effect on the fibre composition and biodegradability

TP were composed above all by recalcitrant fibers (ADL) attributable to the lignin, cutine, suberine of the tomato seed coats (Taylor and Salenka, 2012) plus hemicellulose and cellulose from peel; then the remaining fraction was the more easily degradable component (CS) made up mainly of oil and protein from the seeds (Del Valle et al., 2006) (Table 2). Although highly recalcitrant fibres formed the larger part of the TP, TP_{rawIM} had medium-high ABP value comparable with other biomasses employed as AD plant feed (Schievano et al., 2009), thanks to the oil and protein fractions' high specific biogas production (ABP_{oil} =950 Nl kg^{-1} d.m. and $ABP_{protein}$= 570 Nl kg^{-1} d.m.) (Wilkie, 2008).

Except for the S_{rawIM} CS, that depended on the oil extraction yield, TP-SFE-CO_2 did not determine macromolecular compositional changes, therefore for TP_{exh} a significant ABP reduction was expected and calculable by using the oil extract and ABP_{oil} as follows: ABP_{TPexh}= [(ABP_{oil}*oil extract (g)/1000] (Table 2). Experimental TP_{exh} ABP not only disagreed with theoretical data (ABP S_{exh} = 234Nl kg^{-1} d.m. and ABP A_{exh}= 220 Nl kg^{-1} d.m.) but were even higher than the TP_{rawIM} meaning that

despite the TP_{exh} recalcitrant fraction being more concentrated than in TP_{rawIM}, biomass biodegradability increased after TP-SFE-CO_2. The vegetal structural damage occurred during TP-SFE-CO_2 can lead to higher fibre bioavailability that did not depend on macromolecular concentration but rather on the fibre organization (Carpita and McCann, 2000) (Fig. 2, 3).

A first attempt to get phenomenon quantification was tried by calculating the biogas specific fibre production (ABP_{fibre}) before and after TP-SFE-CO_2 (Table 2). To do so, TPs were considered to be composed with a good approximation by fibre (ADL+hemicellulose+cellulose) + oil + protein. Knowing TP_{rawIM}, TP_{exh}, oil and protein amounts and oil and protein specific ABP production, ABP_{fibre} were estimated as $ABP_{TPrawIM\ or\ exh}$ – [(ABP_{oil} * $oil_{rawIM\ or\ exh}$ (g)/1000) + ($ABP_{protein}$*$protein_{rawIM\ or\ exh}$ (g)/1000)]. The ABP_{fibre} was equal to 267 Nl kg^{-1} d.m. and 252 Nl kg^{-1} d.m. for the S_{rawIM} and A_{rawIM} then values became 406 Nl kg^{-1} d.m. and 365 Nl kg^{-1} d.m. for the S_{exh} and A_{exh} respectively that corresponded to an average biodegradability increase of 64%. This result agreed with previous works that described an increase of fibre availability measured as sugars-free fraction (Kehili et al., 2016).Ionic liquid (IL) was already able to improve fibre biodegradability, however exhaust biomass was IL polluted and unusable as AD feedstock (Allison and Simmons, 2017). On the contrary, SFE-CO_2 gave exhaust biomass solvent-free, dried and sterilised, characteristics that improved TP_{exh} re-usability respect to the TP_{raw}.

3.6. Biorefinery mass balance and economic feasibility

Experimental data of this work were used to define the best TP-SFE-CO_2 process to get the maximum extraction yield possible. Results highlighted how not only the SFE-CO_2 parameters but also biomass properties (i.e. moisture, vegetal tissue morphology) are fundamental to reach high lyc recovery.

The experimental conditions adopted for A_{raw} guaranteed a better recovery than those applied for $S_{raw;}$ they were therefore applied to the biorefinery design.

With the aim to evaluate the economic feasibility of the process, experimental data (Table 2, Table 3) were applied to a typical tomato processing plant located in Emilia Romagna (North Italy), one of the most productive areas dedicated to the tomato cannery industry.

The tomato cannery plant has as an input of 60,000 t y^{-1} of tomato, that produced 1,800 t w.w. TP after industrial transformation. Actually TP_{raw} are destined to a near AD plant to integrate the feedstock intake commonly made by maize silage, a dedicated energy crops-EC which employment ().garanteed high biogas production (ABP=250 Nm^3 ton^{-1} w.w.) but was scarcely sustainable for the cultivation environmental and economic costs (Schievano et al., 2015; Paudel et al., 2019; Hol-Nielsen et al., 2009).

Due to low ABP (ABP=73 Nm^3 ton^{-1} w.w.) respect to the maize silage (ABP pf TP_{raw}=29% of ABP silage maize) and the limited storability, TP_{raw} was not considered a valuable AD feedstock and tomato cannery paid 10 € ton^{-1} w.w. TP transport to AD plant (transportation cost=18*10^6 € y^{-1}).

By introducing the TP-SFE_CO_2 step there will be the production of 50.684 kg y^{-1} extract that, considering a lyc concentration of 833 mg kg^{-1} extract, corresponds to 42.22 kg y^{-1} lyc.

The feasibility of the new biorefinery was estimated taking into consideration the cost of manufacturing (COM) and the final product value. The COM was calculated considering the fixed capital investment (FCI), cost of operational labour (C_{ol}) and cost of utilities (C_{ut}) by applying the equation COM=0.28*FCI+2.73*Col+1.23*Cut (Attard et al., 2016; Cristóbal et al., 2018) (see SI).

The elaboration allowed the estimate of the energetic needs and of the expenses for the production (SI). The A_{rawIM}_SFE_CO_2 has a COM of 1,148,360 € y^{-1} that corresponded to 21.28 € kg^{-1} extract in agreement with those found for other carotenoids extraction (Pereira and Meireles, 2010).

To guarantee a prompt biorefinery integration into the local production system, the possibility to destine the A_{exh} to AD processes was evaluated. A_{exh} had a ABP of 360 Nm^3 ton^{-1} w.w. that was around 5 times higher respect to that of TP_{raw} and 1.44 times higher than that of maize silage. This change depended by the moisture reduction ad biodegradability increase occurred during first biorefinery steps (dryng+SFE-CO_2) that transformed TP_{raw} into a profitable and more sustainable AD feedstock respect to EC (Hol-Nielsen et al., 2009). Although TP_{exh} had a substitution capability of 1.44 ton^{-1} w.w. maize silage, its economic value was estimated equal of that of silage maize (40 Euro t^{-1} w.w. ton, AD plant North Italy Owner communication) that, considering the A_{exh} amount (359.72 t w.w. y^{-1}) gave to the tomato cannery plant a potential economical revenue of + 14389 € y^{-1}.

The use of the TP_{exh} gave a theoretical biogas production of 129,648 Nm^3 y^{-1} that corresponded to 62,037 Nm^3 y^{-1} of methane, electric power productivity of 244,493 Kwh y^{-1} and digestate as by-product (Schievano et al., 2015). Digestate is a biological stabilized, mature and sanitized biomass that has optimal composition to produce fertilizers (Tambone et al., 2010; Riva et al., 2016). In this perspective the solid/liquid separation is a commune refining treatment already applied to obtain N and N:P fertilizer respectively employable in substitution to those chemically synthetized as well as encouraged by the new EU Fertilising Product Regulation (European Biogas Association, 2019).

The economical sustainability of the process is directly linked to the market price of the product. Lycopene showed very different market values that depend on the source, production systems, lyc concentration and physical state (crystalline or oleoresin). The high cost difference depends on the origin (synthetic or natural) and on the fact that a natural extract contains several bioactive

molecules. From chemical synthesis or from tomato solvent extraction plus purification, lyc crystalline product are available at costs of 3,000 € kg^{-1} lyc (BCC Research, 2018). A different kind of product are tomato oleoresin, in which in addition to the lyc, there is a vast array of bioactive compounds (*i.e.* carotenoids, vitamins and phytosterols) which price is 50 € kg^{-1} extract characterized by a lyc concentration of 1% that means a price of 5,000 € kg^{-1} lyc.

Previous data did not take into consideration the SFE-CO_2 production system since presently, at the best of our knowledge, this kind of product is not available on the market. Another aspect that complicate the lyc price from SFE_CO_2 price estimation is the different isomers composition in respect to synthetic and solvent-extract products that influenced the bioavailability and the final healthiness effect. Synthetic and solvent extract lyc are trans isomers (trans > 90% total lyc) that was less bioavailable than cis form (Boileau and Boileau, 2002), thus lyc mixture isomers composition influences body adsorptive effect; for example for lyc mixture trans:cys of 95:5 and 55:45 a adsorption degree of about 60% and 99% respectively was reported (Unlu et al., 2007).

Basing on the previous consideration and the A_extract lyc characteristics, in this work we consider reasonable giving a price of 50 € kg^{-1} A_extract that corresponded to that of the oleoresin already on the market. This choice came by the fact that the estimation of the real price is actually unpredictable but, using as reference caffeine, for which synthetic, standard and supercritical extraction products are available in the market (de Melo et al., 2014; Pharmacompass. Com, 2016; Sigma-Aldrich web site, 2019), a higher price than that used in this work is reasonable. Therefore taking into account the market price, the extract amount and the COM, the total net revenue for the biorefinery would be 2,552,186 € y^{-1}, meaning a profit of 1,403,826 € y^{-1} that corresponds + 1,418,229 € y^{-1} (+787.9 € t^{-1} TP) respect to the actual TP management system.

4. Conclusion

The TP_SFE_CO_2 biorefinery was made by: TP pre-drying until to reach moisture of 100 g kg^{-1} w.w. TP that resulted an optimal compromise to contain vegetal tissue alteration and at the same time favourite lyc recovery during SFE-CO_2. The extract was an emulsion rich in lycopene with a favourable trans isomer: cis isomer proportion that was estimated to a have a value of 50 € kg^{-1} extract. The SFE-CO_2 acts as efficacious system to increase fibre biodegradability (+64%) and improved the TP_{exh} characteristics to become a valid substituent of the silage maize actually employed to make AD to obtain bioenergy and fertilizers For a North Italy tomato cannery, TP biorefinery built by SFE-CO_2+AD gave an additional economic revenue improving the production system of + 787.9 € ton^{-1} w.w. TP_{exh} respect to the actual system -10 € ton^{-1} w.w. TP_{raw}.

Table 1 TP-SFE-CO_2 process parameter adopted in literature.

Feedstock tipology	Feedstock amount (g)	CO_2 flow (kg h^{-1})	Temperature (°C)	Pressure (MPa)	Extraction time (min)	Solvent ratio (kg CO_2 kg^{-1} feedstock)	Co-solvent (% feedstock weight)	lyc recovery (%lyc feedstock)	reference
Tomato fruit without seeds	10	20.4	40	40	360	n.r.	5, canola oil	n.r.	Saldaña et al., 2010
Tomato skin and pulp	0.5	0.113	45-35	n.r.	30	1600	-	69	Gómez-Prieto et al., 2003
Tomato fruit	3000	8-20	60-70	40-45	480	n.r.	50, powder roasted hazelnut	70	Ciurla et al., 2009
Tomato pulp	3	24.6	50	50	480	n.r.	-	n.r.	Honda et al., 2017
TP	3	0.114	86	34.5	200	91	-	71	Rozzi et al., 2009[b]
	40-50	0.792	80	30	n.r.[a]	130	-	80	Sabio et al., 2003 [b]
	1000	80	80	46	60	80	-	90	Vàgi et al., 2007 [b]
	1.5	0.354	60	30	300	n.r.	-	93	Nobre et al., 2009 [b]
	1	n.r.	60	40	n.r.	n.r.	-	33	Zhang et al.; 2011 [b]

	4	0.142	90	40	210	n.r.	-	56	Machmudah et al., 2012 [b]
	10	0.24	80	40	120	n.r.	-	60	Kehili et al., 2017 [b]
	53	4	55	30	120	n.r.	5, ethanol	54	Baysal et al., 2000 [b]
	n.r.	0.085	100	40	390	n.r.	-	n.r.	Topal et al., 2006 [b]
	12	22.26	80	50	220	n.r.	-	52	Hatami et al., 2019
	20 (peel:seed 50:50)	8	80	30	280	n.r.	-	100	Vallecilla-Yepez and Cftci, 2018
Average value of each extraction parameter		11.6±25	77.4±13.7	37.3±7	211.1±102.6	100.3±26.3			
Extraction condition adopted in this work			80±1	38		103±4			

[a] n.r. not reported

[b] data used to define better extraction condition (see the text).

Table 2. TP chemical and biological characterisation

		S_{raw}	S_{exh}	A_{raw}	A_{exh}
d.m.	g kg^{-1} ww	218 ±0.10[a,b]	970±28.8A	228 ±0.8	974±45A
$d.m._{IM}$[c]		941±15.9bA		897±32bB	
Total lyc	mg kg^{-1} d.m.	5.79±0.31bB[d]	1.78±0.11A	105±0.9aB[d]	1.01±0.2A
Cis isomers composition: All-trans lyc	% total lyc	54	100	67	100
Cis isomers composition: Cis-sum lyc	% total lyc	46	0	33	0
Cis isomers composition: 9,13-cis-lyc	% cis-sum lyc	45	0	9	0
Cis isomers composition: 15-cis-lyc	% cis-sum lyc	9	0	10	0
Cis isomers composition: 13-cis-lyc	% cis-sum lyc	0	0	3	0
Cis isomers composition: 5,13-cis-lyc	% cis-sum lyc	0	0	12	0
Cis isomers composition: 7-cis-lyc	% cis-sum lyc	14	0	39	0
Cis isomers composition: 5,9-cis-lyc	% cis-sum lyc	32	0	27	0
TEAC	mmol $_{Trolox}$ kg^{-1} d.m.	10.8±1.37	7.79±0.98	11.1±1.12	3.45±0.21
CS		375±1.2bA	340±1A	286 ±1.9aA	288±5.4A
oil		102±23bB	25.1±2A	67.4±13aB	30.7±10A
protein[e]	g kg^{-1} d.m.	129 ±11aA	129±8A	140±15bA	148±14A
hemicellulose	g kg^{-1} d.m.	60.9±3.7aA	50±5.4A	75.6±7.7aA	74.2±1.7A
cellulose	g kg^{-1} d.m.	146±4.1aA	150±2.5A	169±3.9bA	172±7.6A
ADL	g kg^{-1} d.m.	418±1.95aA	460±8.8A	470±1.9bA	466±11.3A
ABP	Nl kg^{-1} d.m.	337±3aA	365±2B	324±2bA	370±3B

[a] data followed by the same capital letter in the same line for the same TP-SFE-CO_2 are not statistically different (ANOVA Bootstrap, $p<0.05$)

[b] data followed by the small letter in the same line are not statistically different (ANOVA Bootstrap, $p<0.05$)

[c] $d.m._{IM}$: S_{rawIM} and A_{rawIM} dry matter content reached after partial dehydration step done before SFE-CO_2

[d] Total Lyc concentration determined for the S_{rawIM} and A_{rawIM}

[e] protein content calculated from the NTK *5.7 (Piyakina and Yunusov, 1995)

Table 3. TP-SFE-CO_2 extract characterisation

			S_extract	A_extract
	Total lyc	mg kg^{-1} extract	40±5	619±22
Cis isomers composition	All-trans lyc	% total lyc	23	54
	Cis-sum lyc		77	46
	X di-cis-lyc	% cis-sum lyc	7	0
	9,13'-cis-lyc		36	22
	15-cis-lyc		41	37
	13-cis-lyc		2	1
	5,13-cis-lyc		4	3
	9-cis-lyc		1	23
	7-cis-lyc		0	2
	5,9-cis-lyc		9	12
	TEAC	mmol $_{Trolox}$ kg^{-1} extract	9.62±0.1	27.3±0.59

Caption Figure:

Fig. 1 TP-SFE-CO_2 lyc and extract kinetic trend.

Fig. 2 TP_{rawIM} peel fraction microscopy images: SEM S_{rawIM} (**A**), A_{rawIM} (**B**) cuticle and S_{rawIM} (**C**) and A_{rawIM} (**D**) parenchimatous faces; S_{rawIM} (**E**) and A_{rawIM} (**F**) light microscopy cross-sections in which CW means cell wall; CW ultrastructural TEM micrographs details of (**G**) S_{rawIM} and (**H**) A_{rawIM} where the former showed an expanded CW adjacent to median lamella (ml); scale bars are 20 µm in length (A-D), 10 µm in length (E-F) and 500 nm (G-H).

Fig. 3 TP_{exh} peel fraction microscopy images: SEM S_{exh} (**A**) A_{exh} (**B**) cuticle face in which scratch is (S) and SEM S_{exh} (**C**) and A_{exh} (**D**) parenchimatous faces; Light microscopy cross-sections S_{exh} (**E**) and A_{exh} (**F**); scale bars are 20 µm in length (A-D) and 10 µm in length (E-F).

Fig. 4 Light microscopy images of S_extract **(A)** and A_extract **(B)**. S_extract is yellow uniformly coloured oil with cellular debris and A_extract is dark orange coloured oil with water droplets (W). Confocal microscopy images of the A_extract after labelling of neutral lipid by Nile red **(C)** and phospholipids by Rh-DOPE **(D)**. Black spots are water droplets (W) dispersed in the oil phase (red background). Detail of the phospholipid layer at the oil/water interface (arrow) is enlarged in the panel **(E);** bars are 10 µm in length.

Fig. 1

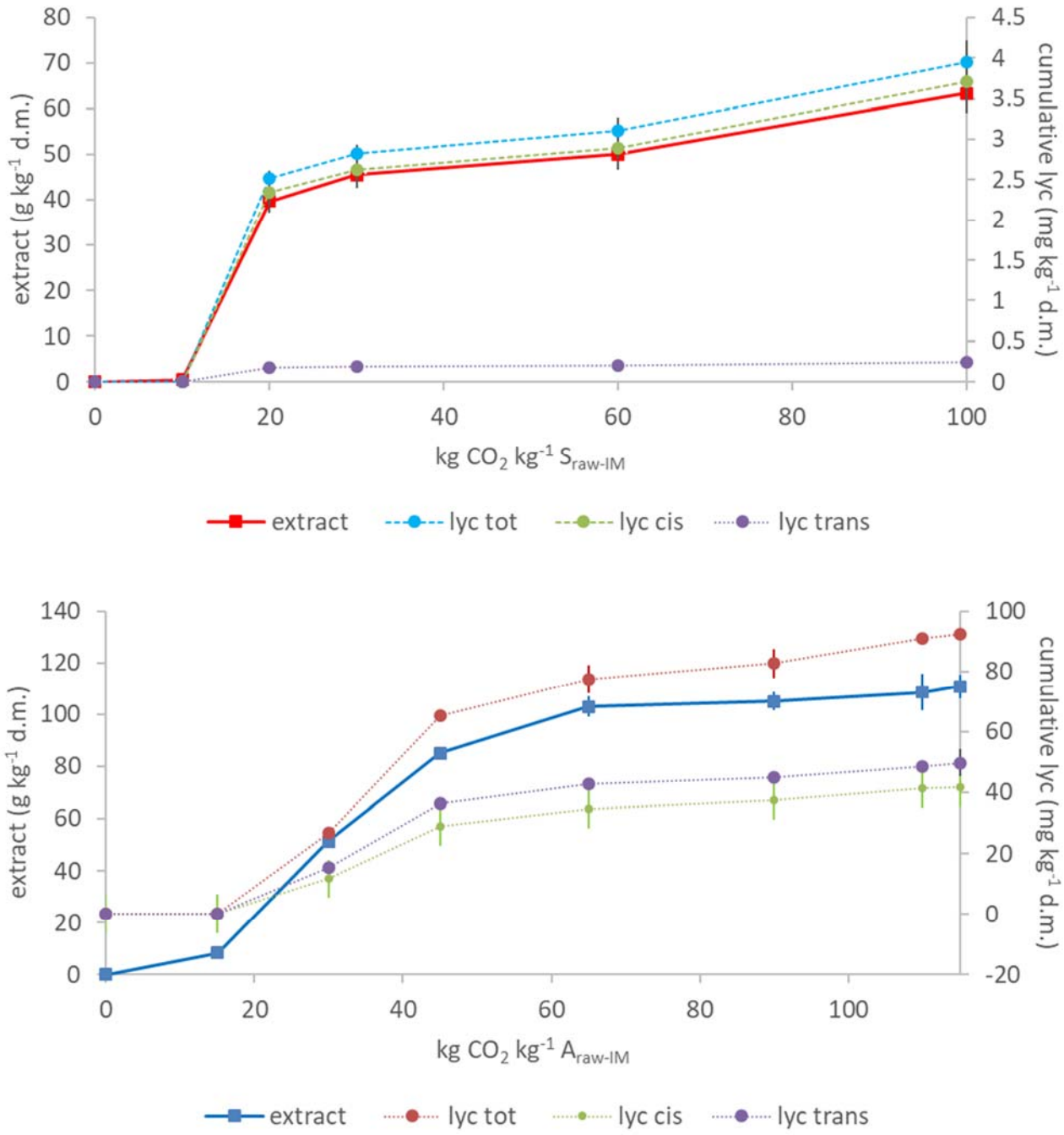
extract (g kg-1 d.m.)
cumulative lyc (mg kg-1 d.m.)
kg CO2 kg-1 Sraw-IM
extract
lyc tot
lyc cis
lyc trans
kg CO2 kg-1 Araw-IM
extract
lyc tot
lyc cis
lyc trans

Fig. 2

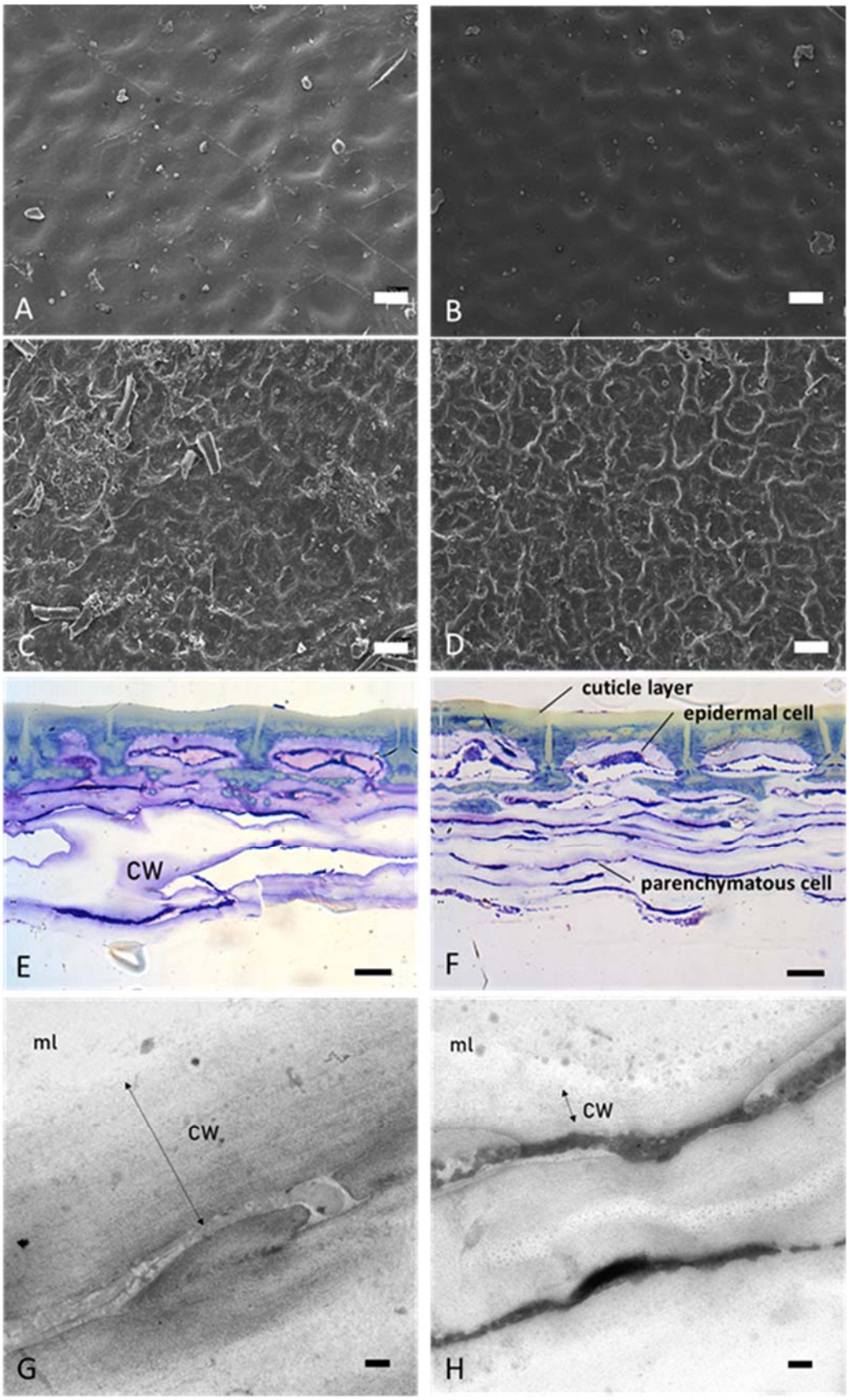
A
B
C
D
cuticle layer
epidermal cell
CW
parenchymatous cell
E
F
ml
CW
ml
CW
G
H

Fig. 3

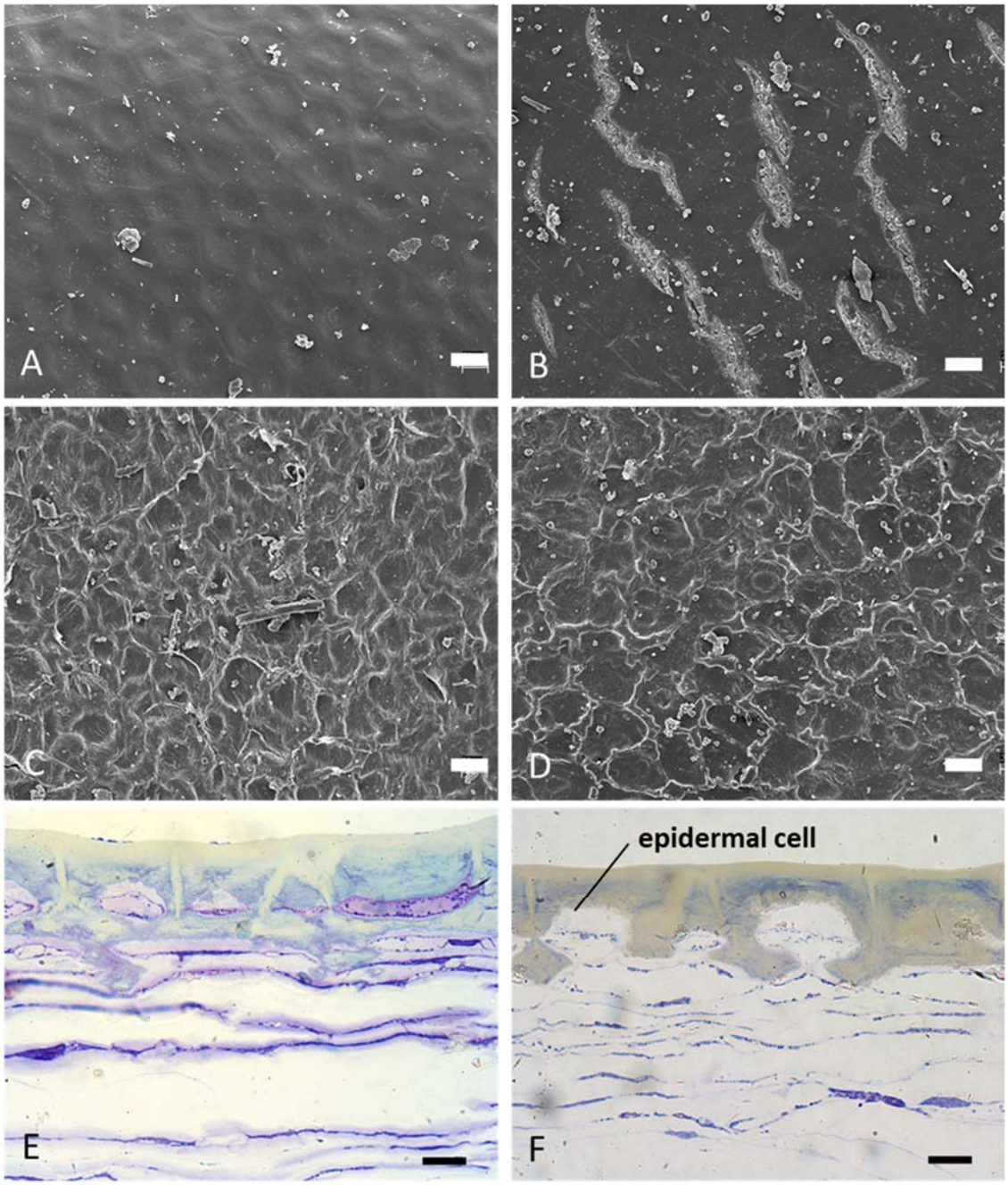

Fig. 4

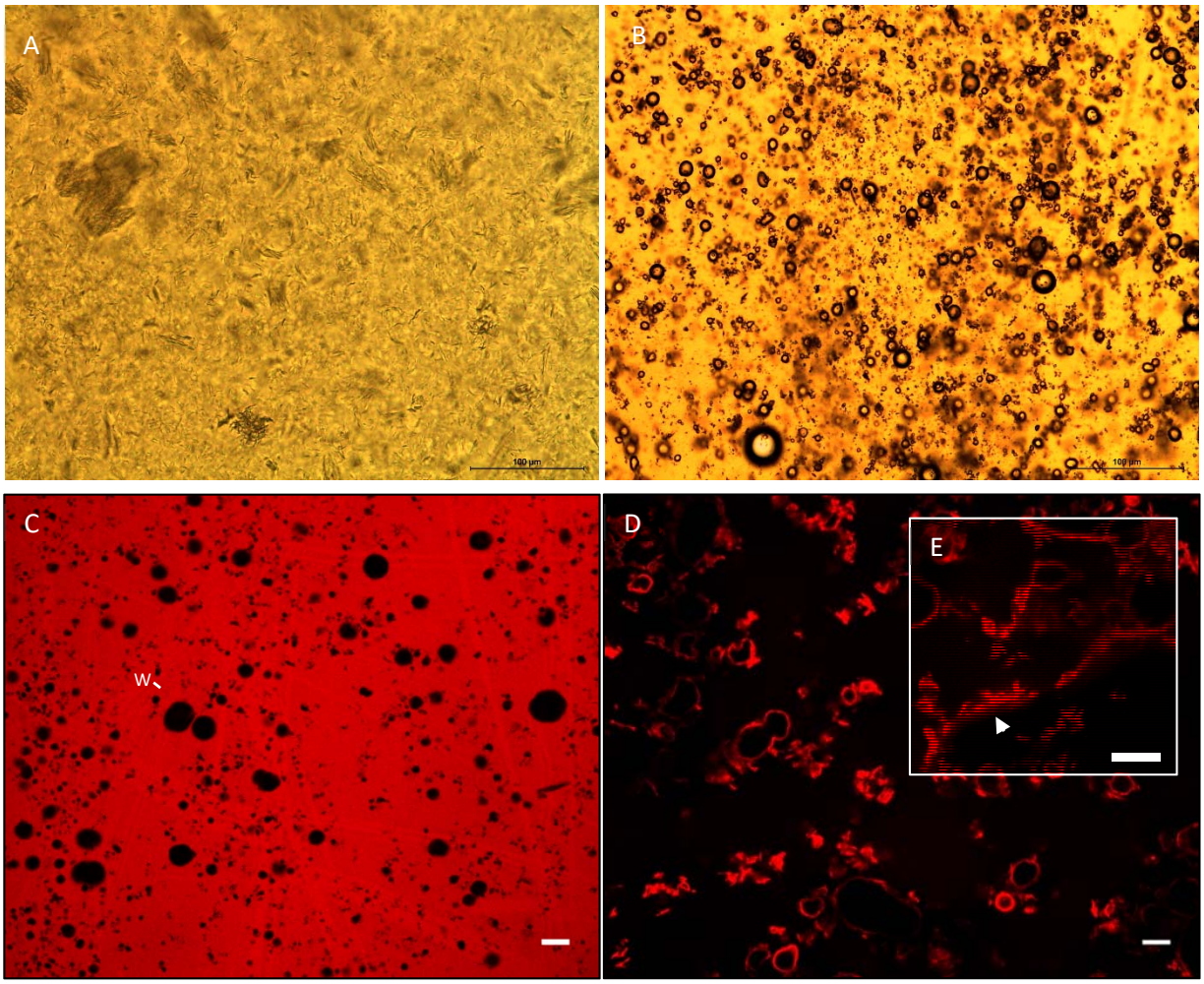

VISUAL ABSTRACT

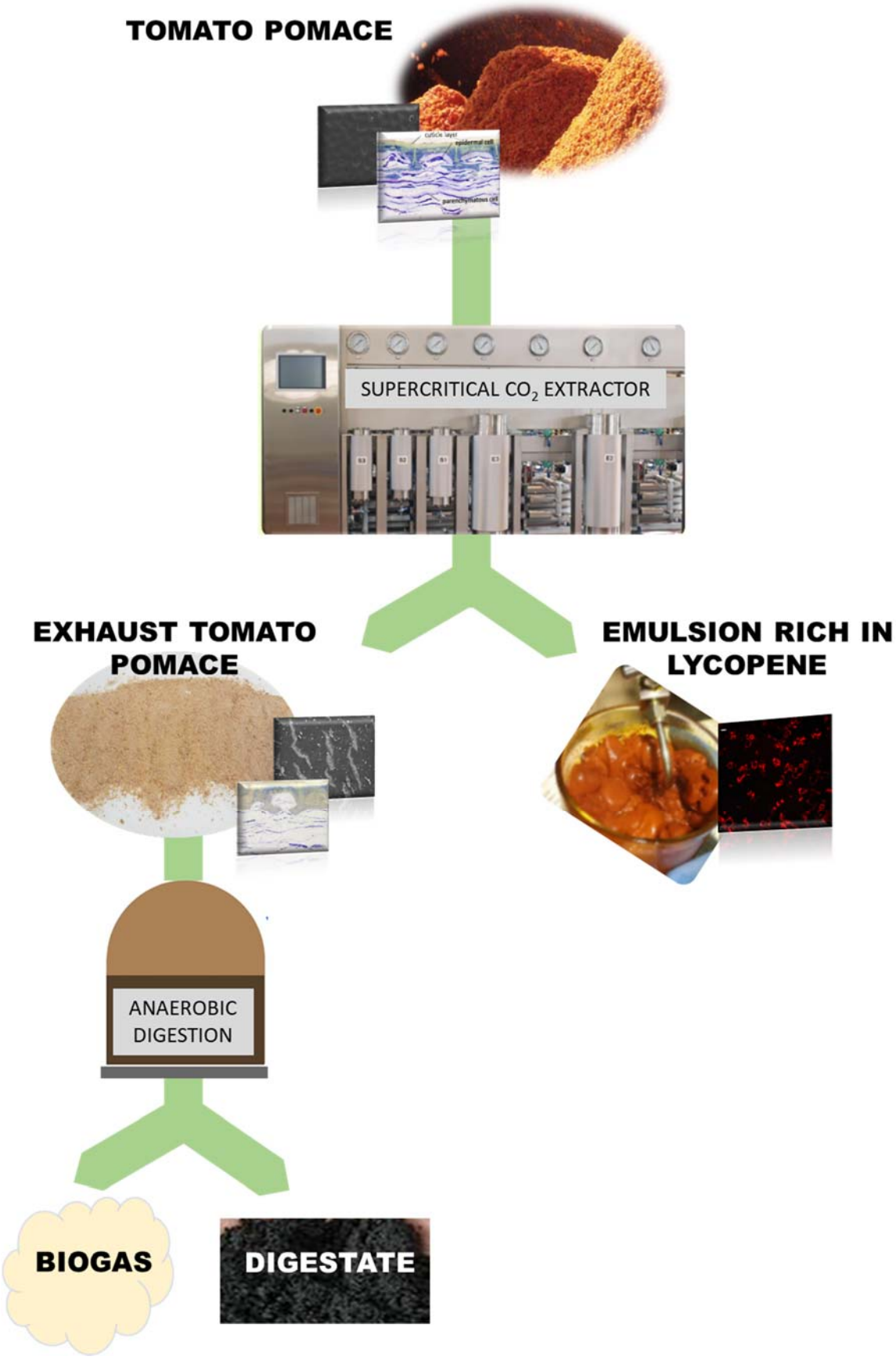

References

Akbudak, B., Bolkan, H., Cohen, N., 2009. Determination of physicochemical characteristics in different products of tomato varieties. Int. J. Food Sci. Nutr. 60, 126-138.

Allison, B. J., Simmons, C. W., 2017. Valorization of tomato pomace by sequential lycopene extraction and anaerobic digestion. Biomass Bioenergy 105, 331-341.

Attard, T. M., McElroy, C. R., Hunt, A. J., 2015. Economic Assessment of Supercritical CO_2 Extraction of Waxes as Part of a Maize Stover Biorefinery. Int. J. Mol. Sci. 16(8), 17546-17564.

Attard, T.M., McElroy, C.R., Gammons, R. J., Slattery, J. M., Supanchaiyamat, N., Kamei, C. L. A., Dolstra, O., Trindade, L. M., Bruce, N. C., McQueen-Mason, S. J., Shimizu, S., Hunt, A. J., 2016. Supercritical CO_2 Extraction as an Effective Pretreatment Step for Wax Extraction in a Miscanthus Biorefinery. ACS Sustainable Chem. Eng**.** 4, 5979−5988.

Baysal, T., Ersus, S., Starmans, D. A. J., 2000. Supercritical CO_2 Extraction of β-Carotene and Lycopene from Tomato Paste Waste. J. Agric. Food Chem. 48, 5507-5511.

BCC Research. 2018. The Global Market for Carotenoids, Wellesley, MA, June 2018. https://www.bccresearch.com/market-research/food-and-beverage/carotenoids-global-market-fod025d.html (available at 27/03/2019).

Boileau, T. W.-M., Boileau, A. C., Erdman, J. W., 2002. Bioavailability of all-trans and cis–Isomers of Lycopene. Exp. Biol. Med. (Maywood) 227- 914.

Breitenbach, J., Braun, G., Steiger, S., Sandmann, G., 2001. Chromatographic performance on a C30-bonded stationary phase of monohydroxycarotenoids with variable chain length or degree of desaturation and of lycopene isomers synthesized by various carotene desaturases. J. Chromatogr. A. 936, 59–69.

Butchosa, N., Leijon, F., Bulone, V., Zhou, Q., 2019. Stronger cellulose microfibril network structure through the expression of cellulose-binding modules in plant primary cell walls. Cellulose 26, 3083-3094.

Carpita, N., McCann, M., 2000. The plant cell wall. In: Biochemistry and Molecular Biology of Plants. American Society Plant Physiologists 52–108.

Ciurlia, L., Bleve, M., Rescio, L., 2009. Supercritical carbon dioxide co-extraction of tomatoes (*Lycopersicum esculentum* L.) and hazelnuts (*Corylus avellana* L.): A new procedure in obtaining a source of natural lycopene. J. Supercrit. Fluids 49, 338–344.

Cristóbal, J., Caldeira, C., Corrado, S., Sala, S., 2018. Techno-economic and profitability analysis of food waste biorefineries at European level. Biores. Technol. 259, 244–252.

Crookes, P. R., Grierson, D., 1983. Ultrastructure of Tomato Fruit Ripening and the Role of Polygalacturonase Isoenzymes in Cell Wall Degradation. Plant Physiol. 72(4), 1088–1093.

de Melo, M. M. R., Barbosa, H. M. A., Passos, C. P., Silva C. M., 2014. Supercritical fluid extraction of spent coffee grounds: measurement of extraction curves, oil characterization and economic analysis. J. Supercrit. Fluids 86, 150-159.

Del Valle, M., Cámara, M., Torija, M.-E., 2006. Chemical characterization of tomato pomace. J. Sci. Food Agric. 86(8), 1232-1236.

D'Incecco, P., Ong, L., Pellegrino, L., Faoro, F., Barbiroli, A., Gras, S., 2018. Effect of temperature on the microstructure of fat globules and the immunoglobulin-mediated interactions between fat and bacteria in natural raw milk creaming. J. Dairy Sci. 101(4), 2984-2997.

Egydio, J. A., Moraes, Â. M., Rosa, P. T. V., 2010. Supercritical fluid extraction of lycopene from tomato juice and characterization of its antioxidation activity. J. Supercrit. Fluids, 54, 159-164.

European Biogas Association, 2019. Overview on key EU policies for the biogas sector. consulted in 08/2019, available from http://european-biogas.eu/2019/02/06/overview-on--key-eu-policies-for-the-biogas-sector/.

Fiori, L., Basso, D., Costa, P., 2009. Supercritical extraction kinetics of seed oil: A new model bridging the 'broken and intact cells' and the 'shrinking-core'models. J. Supercrit. Fluids 48, 131-138.

Floros, J. D., Chinnan, M. S., 1988. Microstructural Changes During Steam Peeling of Fruits and Vegetables. J. Food Sci. 53, 849-853.

Ge, Y., Yan, H., Hui, B., Ni, Y., Cai Wang, S., Cai, T., 2002. Extraction of Natural Vitamin E from Wheat Germ by Supercritical Carbon Dioxide. J. Agric. Food. Chem. 50, 685-689.

Gómez-Prieto, M. S., Caja, M. M., Herraiz, M., Santa-Marìa, G., 2003. Supercritical Fluid Extraction of all-trans-Lycopene from Tomato. J. Agric. Food Chem. 51, 3-7.

Hatami, T., Meireles, M. A. A., Ciftci, O. N., 2019. Supercritical carbon dioxide extraction of lycopene from tomato processing by-products: Mathematical modeling and optimization. J. Food Eng. 241, 18-25.

Honda, M., Watanabe, Y., Murakami, K., Takemura, R., Fukava, T., Wahyudiono, Kanda H., Goto M., 2017. Thermal isomerization pre-treatment to improve lycopene extraction from tomato pulp. LWT 86, 69-75.

Hubbe, M. A., Rojas, O. J., 2008. Colloidal stability and aggregation of lignocellulosic materials in aqueous suspendsion: a review. BioResources, 3, 1419-1491.

Huang, S., Makarema, M., Kiemle, S. N., Zheng, X., He, X., Ye, D., Gomez, E. W., Gomez, E. D., Cosgrove, D. J., Kim, S. H., 2018. Dehydration-induced physical strains of cellulose microfibrils in plant cell walls. Carbohyd. Polym., 197, 337-348.

Kehili, M., Kammlott, M., Choura, S., Zammel, A., Zetzl, C., Smirnova, I., Allouched, N., Sayadi, S., 2017. Supercritical CO_2 extraction and antioxidant activity of lycopene and β-carotene-enriched oleoresin from tomato (*Lycopersicum esculentum* L.) peels by-product of a Tunisian industry. Food Bioprod. Process. 102, 340–349.

Kehili, M., Schmidt, L. M., Reynolds, W., Zammel, A., Zetzl, C., Smirnova, I., Allouche, N., Sayadi, S., 2016. Biorefinery cascade processing for creating added value on tomato industrial by-products from Tunisia. Biotechnol. Biofuels 9, 261-273.

Li, X., Pan, Z., Atungulu, G. G., Wood, D., McHugh, T., 2014. Peeling mechanism of tomato under infrared heating: Peel loosening and cracking. J. Food Eng. 128, 79-87.

Li, X., Pan, Z., Zang, A., Atungulu, G. G., Delwiche, M., Milczarek, R., Wood, D., Williams, T., McHugh, T., Pan, Z., 2014b. LTW- Effects of infrared radiation heating on peeling performance and quality attributes of clingstone peaches. Food Sci. Technol. 55, 34-42.

Liu, G., Hu, X., Gong, Y., He, L., Gao, Y., 2011. Effects of supercritical CO_2 extraction parameters on chemical composition and free radical-scavenging activity of pomegranate (*Punica granatum* L.) seed oil. Food Bioprod. Process. 90, 573-578.

Longo, C., Leo, L., Leone, A., 2012. Carotenoids, fatty acid composition and heat stability of supercritical carbon dioxide-extracted-oleoresins. Int. J. Mol. Sci. 13(4), 4233–4254.

Machmudah, S., Zakaria, S. Winardi, M. Sasaki, M. Goto, N. Kusumoto, Hayakawa K., 2012. Lycopene extraction from tomato peel by-product containing tomato seed using supercritical carbon dioxide. J. Food Eng. 108, 290–296.

Mayeaux, M., Xu, Z., King, J. M., Prinyawiwatkul, W., 2006. Effects of cooking conditions on the lycopene content in tomatoes. J. Food. Sci., 71:461–464.

Müller, L., Fröhlich, K., Böhm, V., 2011. Comparative antioxidant activities of carotenoids measured by ferric reducing antioxidant power (FRAP), ABTS bleaching assay (αTEAC), DPPH assay and peroxyl radical scavenging assay. Food Chem. 129, 139-148.

Mutsokoti, L., Panozzo, A., Pallares, A., Jaiswal, S., Van Loey, A., 2017. Carotenoid bioaccessibility and the relation to lipid digestion: A kinetic study. Food Chem. 232, 124-134.

Nobre, B. P., Palavra, A. F., Pessoa, F. L. P., Mendes, R. L., 2009. Supercritical CO_2 extraction of trans-lycopene from Portuguese tomato industrial waste. Food Chem. 116, 680-685.

Ollanketo, M., Hartoneb, K., Riekkola, M. L., Holm, Y., Hiltunen, R., 2001. Supercritical carbon dioxide extraction of lycopene in tomato skins. Eur. Food. Res. Technol. 212, 561-565.

Pereira, C.G., Meireles, M.A.A., 2010. Supercritical fluid extraction of bioactive compounds: fundamentals, applications and economic perspectives. Food Bioprocess Technol. 3, 340-372.

Perrechil, F. A., Leonardi, G. R., Friberg, S. E., 2014. In: Microscopy: advances in scientific research and education (A. Méndez-Vilas, Ed.) Formatex, 1037-1042.

Pharmacompass. Com, 2016, consulted in 01/2019, available from https://www.pharmacompass.com/price/caffeine.

Piyakina, G. A., Yunusov, T. S., 1995. General characteristics of the proteins of tomato seed flour and tomato skin flour. Chem. Nat. Compd. 31, 495-496.

Richelle, M., Lambelet, P., Rytz, A., Tavazz, I., Mermoud, A.-F., Juhel, C., Bore,l P., Bortlik, K., 2012. The proportion of lycopene isomers in human plasma is modulated by lycopene isomer profile in the meal but not by lycopene preparation. Br. J. Nutr. 107, 1482-1488.

Riva, C., Orzi, V., Carozzi, M., Acutis, M., Boccasile, G., Lonati, S., Tambone, F., D'Imporzano, G., Adani, F., 2016. Short-term experiments in using digestate products as substitutes for mineral (N) fertilizer: Agronomic performance, odours, and ammonia emission impacts. Sci. Total Environ. 547, 206–214.

Rozzi, N. L., Singh, R. K., Vierling, R. A., Watkins, A., 2002. Supercritical Fluid Extraction of Lycopene from Tomato Processing Byproducts. J. Agric. Food Chem. 50, 2638-2643.

Sabio, E., Lozano, M., Montero de Espinosa, V., Mendes, R. L., Pereira, A. P., Palavra, A. F., Coelho, J., 2003. Lycopene and β-Carotene Extraction from Tomato Processing Waste Using Supercritical CO_2. Ind. Eng. Chem. Res. 42, 6641-6646.

Saldaña, M. D. A., Temelli, F., Guigard, S. E., Tomberli, B., Gray, C. G., 2010. Apparent solubility of lycopene and b-carotene in supercritical CO_2, CO_2 + ethanol and CO_2 + canola oil using dynamic extraction of tomatoes. J. Food Eng. 99, 1–8.

Scaglia, B., Tambone, F., Corno, L., Orzi, V., Lazzarini, Y., Garuti, G., Adani, F., 2018. Potential agronomic and environmental properties of thermophilic anaerobically digested municipal sewage sludge measured by an unsupervised and a supervised chemometric approach. Sci. Total Environ. 637-638, 791-802.

Saini, R. K., Keum, Y.-S., 2018. Carotenoid extraction methods: A review of recent developments. Food Chemistry, 240, 90-103.

Schievano, A., D'Imporzano, G., Adani, F., 2009. Substituting energy crops with organic wastes and agro-industrial residues for biogas production. J. Environ. Manage. 90, 2537–2541.

Scoma, A., Rebecchi, S., Bertin, L., Fava, F., 2016. High impact biowastes from South European agro-industries as feedstock for second-generation biorefineries. Crit. Rev. Biotechnol. 36, 175-189.

Shi, J., Kassama, L., Kakuda, Y., 2006. In: Functional food ingredients and nutraceuticals: processing technology. Ed. J. Shi, CRC Press, USA. 45-73. DOI: 10.1201/9781420004076.

Shi, J., Laguer, M. L., Kakuda, Y., Liptay, A., Niekamp, F., 1999. Lycopene degradation and isomerization in tomato dehydration. Food Res. Int. 31, 15-21.

Shi, J., Maguer, M., 2000. Lycopene in tomatoes: chemical and physical properties affected by food processing. Crit. Rev. Biotechnol. 40, 1-42.

Shi, J., Xue, S. J., Jiang, Y., Ye, X., 2009. Supercritical-fluid extraction of lycopene from tomatoes. in: Separation, extraction and concentration processes in the food beverage and nutraceutical industries. 1, 619-645.

Shi, J., Yi, C., Xue, S. J., Jiang, Y., Ma, Y., Li, D., 2009. Effects of modifiers on the profile of lycopene extracted from tomato skins by supercritical CO_2. J. Food Eng., 93, 431-436.

Sigma-Aldrich, consulted in 01/2019, available from https://www.sigmaaldrich.com/catalog/product/aldrich/w222402?lang=it&region=IT.

Szymańska-Chargot, M., Chylińska, M., Gdula, K., Koziol, A., Zdunek, A., 2017. Isolation and characterization of cellulose from different fruit and vegetable pomaces. Polym., 9, 945-961.

Tambone, F., Scaglia, B., D'Imporzano, G., Schievano, A., Orzi, V., Salati, S., Adani, F., 2010. Assessing amendment and fertilizing properties of digestates from anaerobic digestion through a comparative study with digested sludge and compost. Chemosphere 81, 577–583.

Tambone, F., Orzi, V., D'Imporzano, G., Adani, F., 2017. Solid and liquid fractionation of digestate: Mass balance, chemical characterization, and agronomic and environmental value. Biores. Technol., 243, 1251-1256.

Taylor, A.G., Salanenka, Y.A., 2012. Seed treatments: phytotoxicity amelioration and tracer uptake. Seed Sci. Res. 22, 86–90.

The US Composting Council, 1997. In: Test Methods for the Examination of Composting and Compost, 7-15–7-33.

Topal, U., Sasaki, M., Goto, M., Hayakawa, K., 2006. Extraction of lycopene from tomato skin with supercritical carbon dioxide: effect of operating conditions and solubility analysis. J. Agric. Food Chem. 54, 5604 – 5610.

Unlu, N. Z., Bohn, T., Francis, D. M., Nagaraja, H. N., Clinton, S. K., Schwartz, S J., 2007. Lycopene from heat-induced cis-isomer-rich tomato sauce is more bioavailable than from all-trans-rich tomato sauce in human subjects. Br. J. Nutr. 98, 140-146.

Urbonaviciene, D., Viskelis P., 2017. The cis-lycopene isomers composition in supercritical CO_2 extracted tomato by-products. J. Food Sci. Technol. 85, 517-523.

Vàgi, E., Simàndi, B., Vásárhelyiné, K. P., Daood, H., Kéry, Á., Doleschall, F., Nagy, B., 2007. Supercritical carbon dioxide extraction of carotenoids, tocopherols and sitosterols from industrial tomato by-products. J. Supercrit. Fluids 40, 218–226.

Vallecilla-Yepez L., Ciftci N. O., 2018. Increasing cis-lycopene content of the oleoresin from tomato processing byproducts using supercritical carbon dioxide. LWT Food Sci. Tech., 95, 354-360.

Van Soest, P.J., Robertson, J.B., Lewis, B.A., 1991. Methods for dietary fiber, neutral detergent fiber, and nonstarch polysaccharides in relation to animal nutrition. J Dairy Sci. 74(10), 3583-97.

Wilkie, A., 2008. Biomethane from Biomass, Biowaste, and Biofuels. In: Bioenergy. ASM Press, Washington, DC. 195-205.

World Processing tomato council, 2016, https://www.wptc.to/releases-wptc.php (available at 28-03-2019).

Yi, C., Shi, J., Xue, J., Jiang, Y., Li, D., 2009. Effects of supercritical fluid extraction parameters on lycopene yield and antioxidant activity. Food Chem. 113, 1088-1094.

Zhang, K., Jiang, H., Ren, Y., 2011. The Effect of Technical Parameters on Lycopene Extraction in Supercritical Fluid Extraction From Freeze-Dried Tomato Pomace (Peels and Seeds). Adv. Mater. Res. 236-238, 2868-2871.

Zunik, M. H., Norulaini, N. A. N., Omar, A. K. M., 2012. Supercritical carbon dioxide extraction of lycopene: a review. J. Food Eng., 112, 253-262.

Supporting Information

Development of a tomato pomace biorefinery based on a CO_2-supercritical extraction process for the production of a high value lycopene product, bioenergy and digestate.

Barbara Scaglia[a,*], Paolo D'Incecco[b,*], Pietro Squillace[a], Marta Dell'Orto[a], Patrizia De Nisi[a], Luisa Pellegrino[b], Alfondo Botto[c], Cristiano Cavicchi[d], Fabrizio Adani[a].

[a] *Ricicla Group labs- Dipartimento di Scienze Agrarie e Ambientali - Produzione, Territorio, Agroenergia- University of Milan, Milan, Italy;*

[d] *Dipartimento di Scienze per gli Alimenti, la Nutrizione, - University of Milan, Milan, Italy;*

[c] *Exenia Group, Via Carlo Borra 33/35, Pinerolo, Turin, Italy;*

[d] *Gruppo Cavicchi- XII Morelli, Ferrara, Italy.*

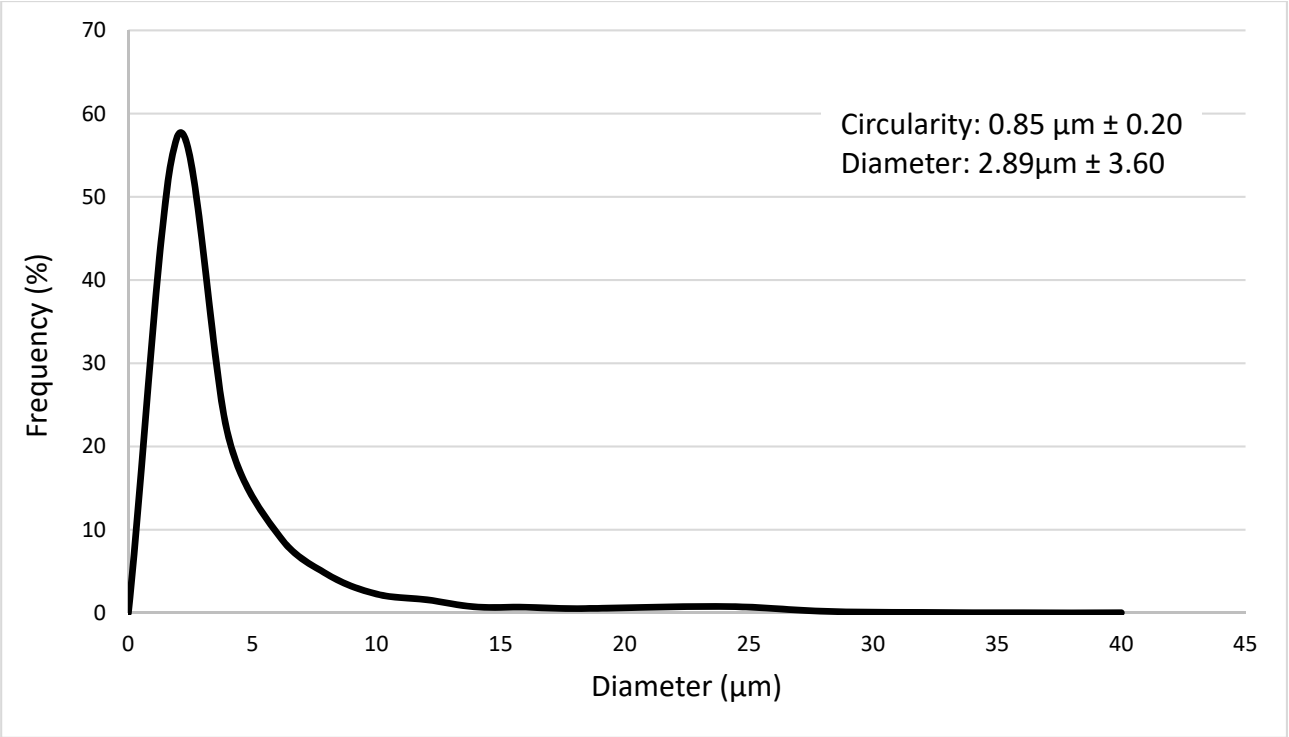

Fig. SI 1. Size distribution of water droplets obtained by image analysis of the CLSM images of the emulsion. Circularity and diameter of the water droplets are expressed as mean ± standard deviation in the panel on the upper right side.

Cost of manufacturing (COM)

To calculate the COM of an industrial process the main type of expenses to consider are the following:

1. Fixed capital investment (FCI): these are constant expenses mainly due to the cost of the apparatus required to carry out the process
2. Cost of operational labour (C_{ol})
3. Cost of utilities (C_{ut})
4. Cost of waste treatment: this parameter can be considered negligible since exhausted TP, the only waste resulting from the extractive process, will be employed to generate heat for the CO_2 heater.
5. Cost of raw material: this parameter can be considered negligible as well since TP is an industrial waste.

The total COM will be calculated with the equation $COM=0.28*FCI+2.73*C_{ol}+1.23*C_{ut}$ (Cristobal et al., 2007).

Fixed capital investment

The industrial supercritical extraction unit employed would be comprised of two 500 l extraction vessels, a CO_2 pump, a CO_2 heater, a refrigerator, and 3 separators (gravimetric, heated cyclonic, cooled cyclonic). The cost of the whole apparatus would be around 2000000 €. The fraction of investment can be calculated by multiplying the total investment by the depreciation rate, assumed to be 10 % per year. The cost of the CO_2 is negligible since the employed gas can be recirculated in the extraction unit.

Operational labour cost

To determine C_{ol}, an hourly salary of 25 € h^{-1} is taken into account (EUROSTAT, 2017a). Considering that for every 6 h cycle an operator must be employed for 2 hours of labor (transporting the TP from the grinder, loading and unloading the extraction vessels), a total of 2640 h y^{-1} of work will be required. Hence, the total C_{ol} will be 66000 € y^{-1}.

Cost of utilities

Five main parameters must be taken into account when estimating the costs of utilities: cost of electricity to dry the TP (C_{ut1}), cost of electricity to grind the TP (C_{ut2}) cost of the electricity used for the CO_2 pump (C_{ut3}), costs associated with the CO_2 heater (C_{ut4}), cost associated with the refrigerator (C_{ut5}). The cost of electricity is considered 0.125 € kWh^{-1} (EUROSTAT, 2017b) and that of gas is 0.0083 € MJ^{-1} (EUROSTAT, 2017d). The flash drier employed consumed 14.5 kWh, while the grinder had an operating power of 5 kWh (Agrindustria Tecco, Cuneo). Considering that the two machines are modules of a single apparatus that can process up to 200 kg h^{-1} (up to a water content of 5 % w. w. $^{-1}$ and a particle size of 0.2 mm), the whole 1800 t of TP can be processed with a total expenditure of 21900 €/y (C_{ut1} + C_{ut2}, 16300 and 5600 € y^{-1} respectively). C_{ut3} can be calculated when pressure, temperature, kg of CO_2 employed per kg of plant material and total dry TP are known: the extractor is operated at 380 bar and 80 °C, at which the specific enthalpy of CO_2 equals 343.16 kJ per kg of CO_2, 103 kg of CO_2 per kg of plant material are used and 457 t of dry TP are processed yearly. Hence, the total C_{ut3} equals 561430 € y^{-1} (CO_2enthalpy*kg_{CO2}*kg_{dry} TP).

C_{ut4} can be calculated by multiplying the heat required in MJ (Q) by the price of gas, following the equation Q=(M*Cp*ΔT)/efficiency. M is the mass of CO_2 recirculated in the apparatus in a year (considering 4 cycles 4 h long per day, with a flow of 15 kg h^{-1} and 330 working days per year), Cp is the specific heat capacity of CO_2 at 80 °C (0.895 kJ kg^{-1}) and ΔT is 76 °C, assuming an efficiency of 50 %, the yearly value of C_{ut4} will be 87000 €.

C_{ut5} is calculated similarly, following the equation Q=M*Cp*ΔT*(COP 4°C)/(COP 20 °C). The fluid (water) required to refrigerate the apparatus has to be cooled from 20 to 4 °C, with a resulting Coefficient Of Performance (COP) of 0.08 and 0.15 respectively. The Cp of CO_2 at 27 °C is 0.846 kJ kg^{-1}. C_{ut5} is calculated similarly, following the equation Q=M*Cp*ΔT*(COP 4°C)/(COP 20 °C).;the fluid (water) required to refrigerate the apparatus has to be cooled from 20 to 4 °C, with a resulting Coefficient Of Performance (COP) of 0.08 and 0.15 respectively thus the Cp of CO_2 at 27 °C is 0.846 kJ kg^{-1} therefore the final value for C_{ut5} will be 71280 € y^{-1}.

References

J. Cristóbal, C. Caldeira, S. Corrado, S. Sala *Biores. Technol.,* 2018, **259**, 244–252

EUROSTAT, 2017a. Electricity price statistics. Available from: http://ec.europa.eu/eurostat/statistics-explained/index.php/Electricity_price_statistics.

EUROSTAT, 2017b. Natural gas price statistics. Available from: http://ec.europa.eu/eurostat/statistics-explained/index.php/Natural_gas_price_statistics.